scientific reports

Check for updates

OPEN

Digital slit lamp derived parameters in shallow anterior chamber screening

Jiahui Zhao[1,2], Xingru He[2], Guangzheng Dai[2], Shenming Hu[3], Xin Zhang[2], Chenguang Zhang[2], Yiting Gong[2], Yibing Zhou[2], Guanghao Qin[2], Shi Chen[2] & Huixin Che[2]✉

To evaluate anterior chamber depth (ACD) using diffraction parameters derived from slit-lamp anterior segment (AS) images and assess their diagnostic efficacy in identifying optimal cutoff values for shallow ACD screening. In this cross-sectional study, from September 21, 2022 to June 30, 2023, 75 volunteers (150 eyes). Slit-lamp images (450 images, 3 pictures per eye) were taken, and the ACD was determined using an IOL Master 700. After manual annotation of the anatomical landmarks, the anterior chamber cross-sectional area (ACCSA) and anterior chamber angle (ACA) of the slit-lamp images were measured. Pixel was applied after image processing and feature extraction to predict the ACD. These values were then compared with the ACD acquired from the IOLMaster 700. The correlation between the parameters of the two techniques was determined by Pearson correlation analysis. The anterior chamber area (ACA) under the receiver operating characteristic curve (AUC) was calculated to evaluate the diagnostic efficacy of relevant indicators on images of the ACD. A total of 450 photographs(207 shallow AC and 243 deep AC images) were analyzed. The nasal/temporal anterior chamber cross-sectional area (N/TACCSA), the sum of the cross-sectional areas of the central and nasal/temporal anterior chambers (SACCSA), and nasal/temporal anterior chamber angle (N/TACA) achieved better performance (AUC = 0.819, 95% confidence interval (CI) = 0.752–0.887; AUC = 0.818, 95% CI = 0.748–0.887 and AUC = 0.833, 95% CI = 0.766–0.899, respectively). The image parameter values were strongly positively correlated with the ACD of IOLMaster 700 (central anterior chamber cross-sectional area (CACCSA, N/TACCSA, SACSA, and N/TACA, *R* = 0.603, 0.651, 0.645, and 0.665, *P* < 0.01, respectively). Some image parameters not only had a strong positive correlation with the measured ACD values from the IOLMaster 700 but also had the ability to screen for shallow ACD. This study suggested the possibility of estimating the central ACD using AS images.

Keywords Anterior segment images, Anterior chamber depth, Digital slit-lamp, Prediction shallow anterior chamber

Angle-closure glaucoma (ACG) accounts for 50% of glaucoma blindness cases worldwide. More than three-quarters of individuals with ACG reside in Asia[1]. In these populations, ACG often develops insidiously, leading to chronically increased intraocular pressure (IOP) and optic nerve damage, and this condition is often asymptomatic and does not receive clinical attention until severe ocular damage has already occurred[2–4]. The prevalence of glaucoma and the rate of blindness among people over 40 years old in China are 2.6% and 30%, respectively. However, ACG is a worldwide problem, and attention should be given to its prevention and diagnosis[5].

Anterior segment (AS) pathologies result from anatomic, structural, or mechanical abnormalities. Clinically, gonioscopy is essential for diagnosing angle closure disease[6]. However, this technique is subjective, has substantial intraobserver and interobserver variability, requires considerable expertise and involves topical anesthesia as well as contact with the cornea[7]. There are currently no standards related to gonioscopy to determine which angles require treatment. All these factors limit the use of gonioscopy in population-based screening[8].

Imaging studies have reported multiple quantifiable angle parameters associated with angle closure[9,10]. The anterior chamber depth (ACD) has been recognized as an important indicator for evaluating the possible closure of the anterior chamber angle. There are many test instruments available for measuring ACD, such as the

[1]Department of Ophthalmology, Jinzhou Central Hospital, No. 51 Shanghai Street, Jinzhou City 121000, China. [2]Department of Ophthalmology, He Eye Specialist Hospital, No. 128 Huanghe North Street, Shenyang City 110001, China. [3]Department of Ophthalmology, Shenyang eye Robo Technology Co., Ltd., No. 128 Huanghe North Street, Shenyang City, China. ✉email: chehuixin@163.com

IOLMaster 700, which is accurate and reliable. However, due to the need for expensive and bulky equipment, the effectiveness of community screening is limited. Ideally, quantitative studies of the anterior chamber and the relationships among its structures could provide objective measurements, which will standardize the anterior chamber (AC) parameters requiring intervention and treatment. Ocular images play a vital role in the clinical diagnosis and individualized treatment of ophthalmic diseases[11–13]. AS images captured using digital slit lamps are expediently obtainable in community screening work and have been widely used in screening for AS diseases.

In our study, we used widely used traditional digital slit-lamp devices to capture AS images and manually annotated two-dimensional features, such as the anterior chamber area (ACA), to determine if features from anterior segment images can be used to identify eyes that have shallow anterior chambers, and are therefore at high risk of angle closure glaucoma.

Methods

This was a cross-sectional, prospective, single-center, clinic-based study. The study protocol adhered to the tenets of the Declaration of Helsinki. This study was approved by the Ethics Committee of Shenyang He Eye Hospital (IRB (2022) K026.01). The participants were recruited after providing written informed consent at the end of their consultation. Images of 150 eyes (207 shallow AC and 243 deep AC images) from 75 volunteers were collected from September 21, 2022, to June 30, 2023.Participants underwent collection of basic demographic and clinical history, including age, sex, and history of ocular trauma or surgery. Intraocular pressure "IOP" was measured using a calibrated Goldmann applanation tonometer, and ACD was assessed via optical biometry with the IOLMaster 700.

Ophthalmic examination

The inclusion criteria for these volunteers were as follows:

- Willing and able to participate in the study.
- Aged between 18 and 80 years old.
- Had not undergone prior intraocular surgery or laser procedures to the eye.
- Be fit enough to keep the eyes open for adequate image acquisition.
- Patients with no concurrent eye pathologies that may obscure photography of the eye.

After providing informed consent, the subject underwent IOLMaster 700 scanning after slit-lamp imaging of the AS.

IOLMaster 700 scanning

IOLMaster 700 scanning was performed by the same professional ophthalmologist in the same environment and equipment (Carl Zeiss Meditec AG, Jena, Germany). We obtained the central anterior chamber depth values of the volunteers, which refers to the distance between the apex of the cornea and the apex of the anterior lens surface, and divided them into groups based on the central ACD (excluding corneal thickness) indicated by the IOLMaster 700: normal group: ACD ≥ 2.5 mm; and shallow AC group: ACD < 2.5 mm.

Image capture protocol

The standard AS images were captured by a digital slit-lamp (SLM-KD4; Topcon, Chongqing, China). Standardized photography indicators and processes: First, a color anterior segment image was captured using a desktop digital slit lamp in a dark room of 15–20 lx. Second, the slit lamp adopted a diffuse lighting method(Virtually all slit lamps incorporate this illumination mode.), with a narrow slit light beam width of 1 mm and a height of 14 mm, with a brightness of 30% of the maximum brightness and no flashing throughout the entire process. Third, the volunteers were asked to be in a head-to-eye position, open their eyes wide, and look straight ahead, and the image clearly showed the entire corneoscleral margin. Fourth, the direct focal illumination method was used, and the light was perpendicular to the subject's central corneal axis. The slit light was fixed to 30°, along the 12 – 6 o'clock meridian axis, corneal nasal/temporal axis (11 – 7 o'clock) and nasal/temporal axis (1–5 o'clock) of the Limbus. As shown in Fig. 1, according to the 3 different positions of the light band, we take 3 images for each eye.

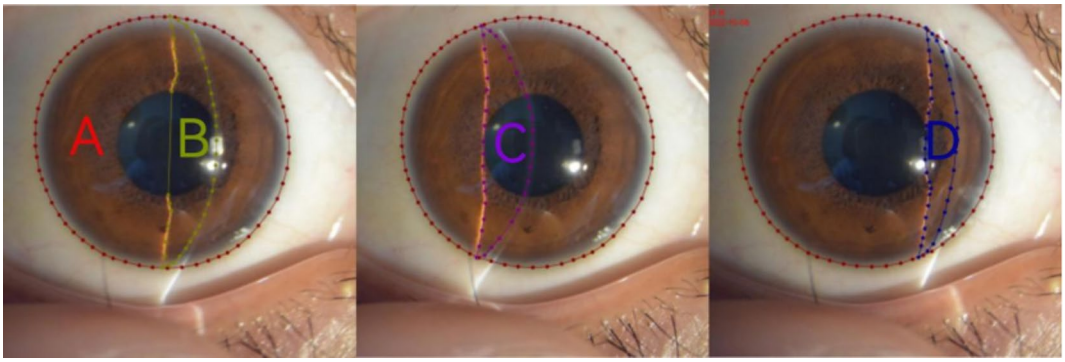

Fig. 1. Landmarks of the AS image about area.

Image feature marking and extraction

The software Labelme (version 4.5.13), developed by MIT's Computer Science and Artificial Intelligence Laboratory, and ImageJ (version V1.8.0.112), developed by the National Institutes of Health, were used for image labeling. The data included the corneal area (A), corneal vertical axis with the slit-light angle fixed to 30° (12 – 6 o'clock) (B), (11 – 7 o'clock) (C), and (1–5 o'clock) (D). As shown in Fig. 1. The angle is measured between the vertex of the corneal light band and the two ends of the iris light band. With the slit-light angle fixed to 30°, the angle of the 12 – 6 o'clock meridian axis is F, the angle of the 11 – 7 o'clock meridian axis is G, the angle of the 1–5 o'clock meridian axis is H. Two light points at the iris root connect to form a straight line as the chord length, and the inner edge of the corneal light band is measured as the arc length. The markings included the following (as shown in Fig. 2): with the slit-light angle fixed to 30°, in the 12 – 6 o'clock meridian axis, arc length (L) and chord length (M) in the cornea nasal/temporal axis (12 – 6 o'clock), arc length (N) and chord length (O) in the cornea nasal/temporal axis (11 – 7 o'clock), and arc length (P) and chord length (Q) in the cornea nasal/temporal axis (1–5 o'clock) were measured. The landmarks were kept consistent for all of the eye images and were annotated for future reference.

The image is binarized to obtain a grayscale image, and image pixels are extracted via Labelme. ImageJ was used to extract the dimensions by measuring the distance, in pixels, between various landmarks of the image.

Image data processing

CACCSA, central anterior chamber cross-sectional area, B/A.

N/TACCSA, nasal/temporal anterior chamber cross-sectional area; (C + D)/2/A.

SACCSA, the sum of the cross-sectional areas of the central and nasal/temporal anterior chambers; CACCSA + N/TACCSA.

N/TACA, nasal/temporal anterior chamber angle, (G + H)/2.

CACA, central anterior chamber angle; F.

CACAB/S, central anterior chamber angle bow/string (B/S), L/M.

N/TACAB/S, nasal/temporal anterior chamber angle bow/string, N/O/2 + P/Q/2.

When performing this calculation, using the ratio of the light band cross-sectional area to the total corneal area as the diffraction parameter provides greater subject-specific accuracy.For both the mean area diffraction parameter and the angular diffraction parameter, measurements were averaged along the 11:00–7:00 and 1:00–5:00 axes.

Statistical analysis

All the statistical analyses were carried out with SPSS version 24.0 (Chicago, IL). The data are expressed as the mean ± SD. Correlation analysis was used to compare the correlation between ACD values measured by the IOLMaster 700 and digital slit lamp image-related parameters (Pearson's test). The correlation coefficient index[14] showed a negligible correlation between 0.00 and 0.10, a weak correlation between 0.1 and 0.39, a moderate correlation between 0.40 and 0.69, a strong correlation between 0.70 and 0.89, and a very strong correlation between 0.90 and 1.0. The image-related parameter indicator optimal threshold was determined from the receiver operating characteristic (ROC) curve using the Youden index (J)[15]. The ability to discriminate between deep AC and shallow AC subjects for continuous data was described using partial area under the receiver operating characteristic (ROC) curve estimates (AUC). The following ROC curves were evaluated: 0.5–0.6, indicating failure; 0.6–0.7, indicating poor recognition ability; 0.7–0.8, indicating fair recognition ability; 0.8–0.9, indicating good recognition ability; and 0.9-1.0, indicating excellent recognition ability. $P < 0.05$ was considered to indicate statistical significance.

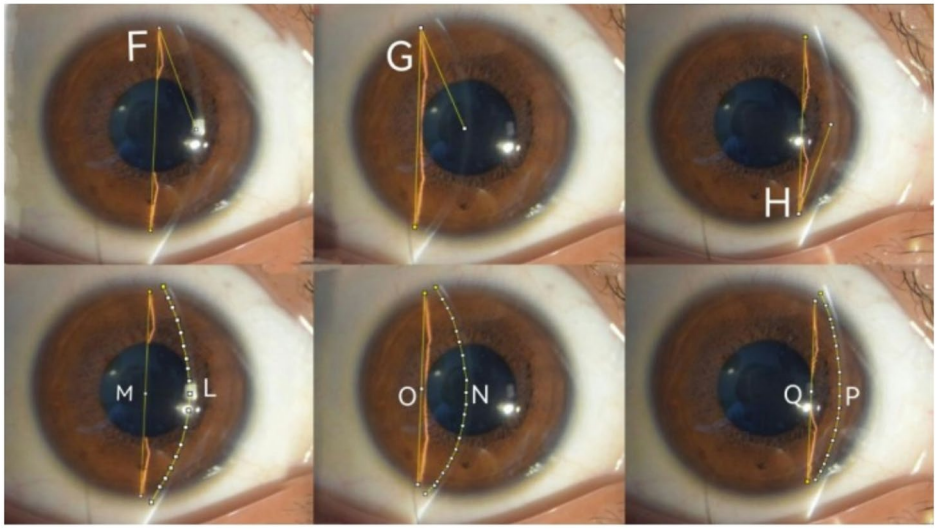

Fig. 2. Landmarks of the AS image about angle and length.

Characteristics	Value	Range
Eye/volunteer (n)	150/75	
Mean age (years)	44.35 ± 17.84	18,78
Male/female sex (n)	33/42	
ACD(mm)	2.559 ± 0.722	
IOP(mmHg)	15.89 ± 4.77	9,21

Table 1. Demographic and ocular characteristics of the participants included in this study. ACD means anterior chamber depth, IOP means intraocular pressure.

	Deep AC	Shallow AC	t	*P* Value
ACD(mm)	3.17 ± 0.56	2.02 ± 0.28	16.38	< 0.01
IOP(mmHg)	14.72 ± 2.70	16.00 ± 3.40	-2.50	0.014

Table 2. Comparison of ocular characteristics between the deep AC group and the shallow AC group. $P < 0.05$ was considered to indicate statistical significance. ACD means anterior chamber depth, IOP means intraocular pressure, AC means anterior chamber.

Comparison between	Mean ± SD	Pearson's *R*	*P*
CACCSA and ACD	0.789 ± 0.038	0.603**	<0.01
N/TACCSA and ACD	0.0534 ± 0.031	0.651**	<0.01
SACCSA and ACD	0.134 ± 0.068	0.645**	<0.01
N/TACA(°) and ACD	17.069 ± 4.362	0.665**	<0.01
CACA(°) and ACD	18.020 ± 4.498	0.566**	<0.01
CACAB/S and ACD	1.127 ± 0.102	0.331**	<0.01
N/TACAB/S and ACD	1.151 ± 0.142	0.268**	<0.01

Table 3. Correlation between AS image parameters and ACD measured by iolmaster 700. ** means $P < 0.001$, $P < 0.05$ was statistically significant. The correlation coefficient index: negligible correlation between 0.00-0.10, weak correlation between 0.1–0.39, moderate correlation between 0.40–0.69, strong correlation between 0.70–0.89, and very strong correlation between 0.90-1.0.AS means anterior segment, ACD means anterior chamber depth. CACCSA means central anterior chamber cross-sectional area. N/TACCSA means The nasal/temporal anterior chamber cross-sectional area. SACCSA means the sum of the cross-sectional areas of the central and nasal/temporal anterior chambers. N/TACA means and nasal/temporal anterior chamber angle. CACA means central anterior chamber angle.CACAB/S means central anterior chamber angle bow/string. N/TACAB/S means nasal/temporal anterior chamber angle bow/string.

Results

A total of 75 volunteers and 150 eyes (450 images) were included; 66 eyes were male (44%), 84 eyes were female (56%), with an average age of 44.35 ± 17.84 years (18–78 years). The mean IOP was 15.56 ± 3.17 mmHg (9–21 mmHg). The mean ACD measured by the IOLMaster 700 was 2.559 ± 0.722 mm. As shown in Tables 1 and 2. Taking the anterior chamber depth of 2.5 cm as the classification criterion. The deep group includes those with chamber depths ≥ 2.5 mm, and the shallow group is those with chamber depths < 2.5 mm. The ACD of the deep AC group was 3.17 ± 0.56 mm, that of the shallow AC group was 2.02 ± 0.28 mm. Similarly, the IOP of the deep AC group was 14.72 ± 2.70 mmHg, that of the shallow AC group was 16.00 ± 3.40 mmHg, and the difference between the two groups was statistically significant (t'=-2.50, $P = 0.014 < 0.05$). In our study, female subjects outnumbered male subjects. This sex distribution is consistent with the globally observed higher prevalence of angle-closure glaucoma ACG among females[16,17].

Correlation analysis was conducted between the ACD measured by the IOLMaster 700 and the relevant parameter indices of the digital slit-lamp image, and the results are shown in Table 3. ACD had a moderate correlation with CACCSA ($r = 0.603$, $P < 0.01$), N/TACCSA ($r = 0.651$, $P < 0.01$), SACCSA ($r = 0.645$, $P < 0.01$), N/TACA ($r = 0.665$, $P < 0.01$), and CACA ($r = 0.566$, $P < 0.01$). The N/TACA correlation is stronger than that of the other indicators. The correlations between the ACD and CACAB/S ($r = 0.331$, $P < 0.01$) and between the ACD and N/TACAB/S ($r = 0.268$, $P < 0.01$) were weak. At the same time, ACD values measured by an IOLMaster 700 (≥ 2.5 mm) were used for binary classification to measure the ability of relevant parameters of digital slit lamp images to judge the depth of the front. The AUC is a measure of the overall performance of a diagnostic test and can be interpreted as the average value of the sensitivities for all possible specificities. The AUC has a value between 0 and 1 but is meaningful as a diagnostic test only when it is > 0.5. The corresponding values are obtained according to the Youden index, as shown in Table 4. The recognition ability of the CACAB/S was poor, the AUC

Variables	AUC	(95% CI)	Youden index	Optimal Cutof	Sensitivity	Sensitivity
CACCSA	0.777	(0.699—0.855)	0.556	0.065	0.672	0.884
N/TACCSA	0.819	(0.752—0.887)	0.536	0.082	0.734	0.802
SACCSA	0.818	(0.748—0.887)	0.583	0.146	0.734	0.849
N/TACA	0.833	(0.766—0.899)	0.552	18.250	0.703	0.849
CACA	0.776	(0.701—0.851)	0.440	18.500	0.719	0.721
CACAB/S	0.684	(0.595—0.773)	0.389	1.128	0.703	0.686
N/TACAB/S	0.720	(0.636—0.804)	0.452	1.140	0.766	0.686

Table 4. Summary of AS image parameters in detection of shallow AC. AS means anterior segment, AC means anterior chamber.AUC means area under the receiver operating characteristic curve.CI means confidence interval.

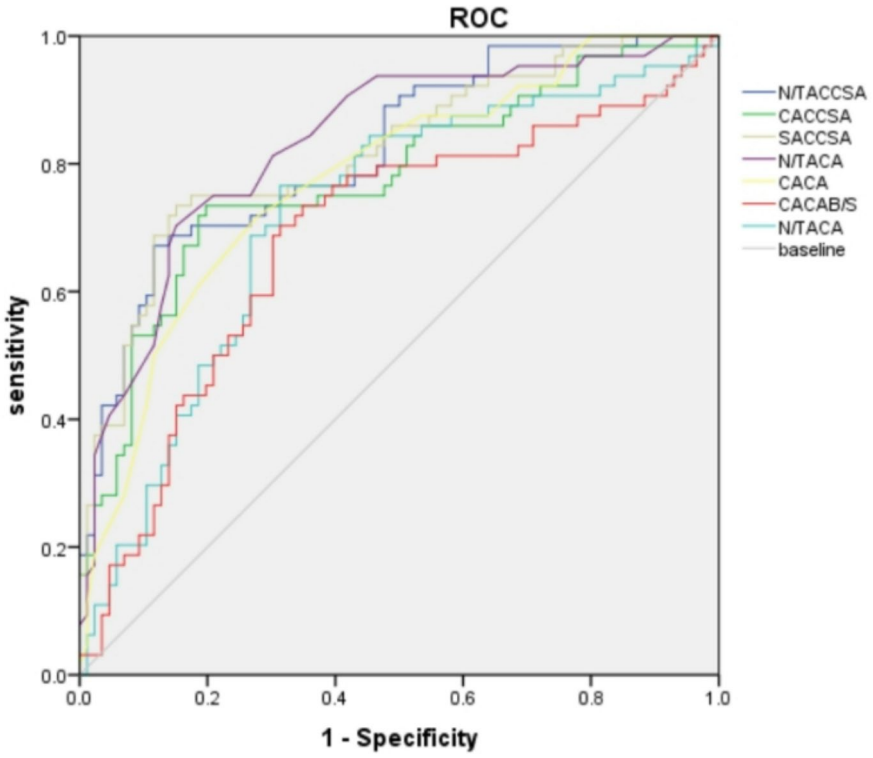

Fig. 3. Receiver operating characteristic for AS image parameters against the shallow AC screening standard.

was 0.684 (95% CI = 0.595–0.773), and the screening threshold for shallow anterior chambers was 1.128. The recognition abilities of CACCSA, CACA, and N/TACAB/S were fair, with AUCs of 0.777 (95% CI = 0.699–0.855), 0.776 (95% CI = 0.701–0.851) and 0.720 (95% CI = 0.636–0.804), respectively, and the screening thresholds for the shallow anterior chamber were 0.065, 18.5 and 0.452, respectively. Notably, N/TACCSA, SACCSA and N/TACA had good recognition abilities, with AUCs of 0.819 (95% CI = 0.752–0.887), 0.818 (95% CI = 0.748–0.887), and 0.833 (95% CI = 0.766–0.899), respectively, and the screening thresholds for the shallow anterior chamber were 0.082, 0.146 and 18.25, respectively. Among them, the N/TACA ratio was the best, with a Yoden index of 0.552, a sensitivity of 70.3%, and a specificity of 84.9%. For a more intuitive comparison, the ROC curve was drawn, as shown in Fig. 3.

Discussion

To effectively prevent ACG by the use of prophylactic laser iridotomy, it is necessary to identify people with early-stage disease. The diagnosis of angle closure disease usually requires clinical examination with a slit lamp, with gonioscopy and additional equipment, including ultrasound biomicroscopy (UBM). Subjective clinical assessments, such as van Herick grading, have only moderate repeatability in trained graders[18,19]. The van Herick method has been proposed as a simple triage test before gonioscopy[20], but it has been reported to have varying sensitivities and specificities, with the lowest being 53%[21] and 57%[4]. UBM measurement of the anterior chamber

angle is objective, but it can cause discomfort to patients and is not suitable for deployment in community settings.

ACD is the main risk factor for angle closure and has been recommended as a rapid screening parameter for ACG[22,23], closely related to the formation of peripheral anterior synechia (PAS). It is easy to manage in large-scale screening and is more intuitively understood and interpreted as a screening parameter[24]. Early clinical identification of a shallow AC can lead to early diagnosis and treatment of ACG.

There are various devices for measuring ACD, including acoustic biometry and optical biometry devices. The IOLMaster 700 is the first swept-source optical coherence tomography (SS-OCT)-based biometric device. Ocular biometric measurements using these devices have shown high accuracy[25]. However, the equipment is large and inconvenient to carry. Importantly, the cost of digital slit lamps is much lower than that of large eye examination devices such as UBM and IOLMaster. Theoretically, community-based screening should be used for which doctors can perform independently, quickly, non-invasively, and with high relevance to the IOLMaster700. AS images are the most readily available, and this device is also used for community screening. Our study is based on simple, accessible and intuitive clinical observation using slit lamp photography.

In our research, using manual annotation of sensitive areas in the section of the image, the indicators for predicting the ACD included the CACCSA, N/TACCSA, and SACSA, which are all two-dimensional data. We use these two-dimensional data indicators for comparison with ACD (one-dimensional data), which is comprehensive, more accurate and less prone to errors. When we processed this part of the data, corresponding attention was given to the details. Accounting for anatomical variations in corneal size associated with inter-subject differences in globe dimensions, using the ratio of the light band cross-sectional area (from slit lamp imaging) to the total corneal area as the diffraction parameter provides enhanced subject-specific accuracy.We also took the average area of the ACA at 11 – 7:00 and 1–5:00. This bilateral averaging approach was employed because the combined error from nasal and temporal quadrant measurements consistently demonstrates less variability than the error observed when using parameters from either quadrant alone. Similarly, when measuring angles, the average value of the surrounding area is also taken to reduce errors. Neither image processing nor the ACD includes corneal thickness. During image processing, the inner edge of the corneal light band is taken for calculation, and the ACD is also calculated from the inner surface of the cornea. At the same time, the light mode has an effect on the pupil size, which affects the marked area. In order to normalize the indicators and reduce errors, we fixed the slit lamp mode during data acquisition and shooting.

It is generally believed that the normal ACD of Chinese people is between 2.5 and 3 cm; in our study, 2.5 cm was used as the cutoff for screening the ACD. A shallow ACD was defined as an ACD less than 2.5 mm and was temporarily considered to be at risk of angular closure. We found that the correlations between the CACCSA, N/TACCSA, SACSA, and N/TACA and the ACD measured by the IOLMaster 700 were stronger, suggesting that the above indicators could be used as screening parameters for the ACD. In our study, both CACCSA and B/TACCSA were acquired as two-dimensional parameters, potentially offering greater accuracy than one-dimensional measurements. Among these, the peripheral measurement indicator N/TACCSA demonstrated a stronger correlation with ACD measured by IOLMaster 700 and proved more representative than other diffraction parameters (such as the central parameter CACCSA). This enhanced representativity translates to improved efficacy in detecting shallow versus deep anterior chambers.A preliminary study in Singapore[26] showed that the predicted ACD values of mobile phone AS images were related to the measured ACD values from AS-OCT. Similar to our research, it has been proven that AS image indicators are related to device measurements of the ACD. The difference between these methods is the use of ACD measurement equipment, such as AS-OCT, while our research used an IOLMaster 700 instrument.

Qian[27] proposed a high-performing deep learning model to automatically detect shallow ACD from overview anterior segment photographs. The ACD is also the distance from the corneal endothelium to the anterior surface of the lens. However, Qian's research focused only on central parameters and ignored the most sensitive peripheral parameters. Our study used precise two-dimensional data to evaluate central and peripheral AC and found that the ability to recognize peripheral area parameters was better.

Our study included AS image angle indicators and found that there was a large disparity in the angle indicators. Although the correlation between the N/TACA, CACA and ACD was moderate ($r = 0.665$ and 0.566, respectively), the N/TACA was the strongest among all AS image indicators. This finding indicated that the change in the central angle was not as significant as that in the peripheral angle. Moreover, the recognition abilities of the two methods are vastly different. N/TACA had the best recognition ability among all indicators, with an AUC of 0.833, a Youden index of 0.552, a sensitivity of 70.3%, and a specificity of 84.9%. This is sufficient to prove that N/TACA has a high diagnostic value and can be used as a screening indicator for the shallow AC. However, the recognition ability of CACA is only fair, with an AUC of only 0.776. Another study used UBM to measure angle parameters related to the anterior segment, such as the trabecular iris angle and sclera-ciliary process angle. Although these indicators are more intuitive, their use is limited, and they are not suitable for screening. It is obvious that angle indicators are very important, and the angle indicators in our research are easy to obtain, which is an advantage. At the same time, these findings also prove that the peripheral angle indicator is more explanatory and can be used as a reference indicator for screening shallow anterior chambers.

Sasan Moghimi's study[28] showed that using AS-OCT to measure the anterior chamber width and posterior corneal arc length of ACG eyes is less common. Our study compared the chord length and arc length in more slit lamp-obtained AS images, which was similar to the findings of Sasan Moghimi's study. This study revealed that both CACAB/S and N/TACAB/S had weak correlations with ACD (r = 0.331 and 0.268, respectively), while their ability to identify shallow AC was also poor (AUC = 0.684 and 0.720, respectively). This may be related to the degree of iris distention and will be further explored in the future. With this pilot study, there is promise for an AI-driven diagnostic capability for ACD screening for a digital slit lamp device. Much attention has been focused on creating a computer-aided diagnosis system based on currently available images and on

enhancing diagnostic accuracy and efficiency[29,30]. Zhi Da Soh 's[31] article predicted ACD from low-cost anterior segment photographs (ASPs) using deep-learning (DL), and our study used anterior segment images to predict shallow anterior chamber structure, both of which have good prediction results. Critically, whereas his study utilized only a single sclerotic scatter illumination image acquired at a fixed angle, my investigation encompasses multiple illumination angles and distinct slit-beam positions, representing significantly more comprehensive parametric variations. This methodological distinction likely underpins our novel findings.

Our study had several limitations. Manual marking of image landmarks by humans could also introduce inaccuracies. Of course, the manual annotation will be further automated in the future to provide convenience for clinical applications .The reference indicator is currently limited to the central ACD in IOLMaster 700 scanning, but the prediction of other anterior chamber parameters, among other devices, would be expected in subsequent studies with larger sample sizes. Additionally, gonioscopy findings and the Smith method were not performed on the subjects in our study. Last, this study was performed on a uniform East Asian population (all volunteers were Chinese) aged 18 years and older; thus, the results may not be generalizable to other dissimilar populations.

In conclusion, our study showed that reference indicators for digital slit lamps such as N/TACCSA, SACCSA, and N/TACA can predict anterior chamber depth and have good recognition ability, allowing for the recognition of ACG and providing reference indicators for community screening.

Data availability

The datasets used and/or analyzed during the current study are available from the corresponding author upon reasonable request.

Received: 28 March 2025; Accepted: 23 September 2025
Published online: 29 October 2025

References

1. Quigley, H. & Broman, A. T. The number of people with glaucoma worldwide in 2010 and 2020. *Br. J. Ophthalmol.* **90**, 262–267 (2006).
2. Foster, P. J. et al. The prevalence of glaucoma in Chinese residents of Singapore: a cross-sectional population survey of the Tanjong Pagar district. *Arch. Ophthalmol. (Chicago, Ill.)* **118**, 1105–1111 (2000) (1960).
3. Foster, P. J. et al. Glaucoma in Mongolia. A population-based survey in Hövsgöl province, northern Mongolia. *Arch. Ophthalmol. (Chicago, Ill.)* 114, 1235–1241 (1996).) 114, 1235–1241 (1996). (1960).
4. Congdon, N. G., Quigley, H. A., Hung, P. T., Wang, T. H. & Ho, T. C. Screening techniques for angle-closure glaucoma in rural Taiwan. *Acta Ophthalmol. Scand.* **74**, 113–119 (1996).
5. Quigley, H. A., Congdon, N. G. & Friedman, D. S. Glaucoma in China (and worldwide): changes in established thinking will decrease preventable blindness. *Br. J. Ophthalmol.* **85**, 1271–1272 (2001).
6. Fu, H. et al. Angle-Closure detection in anterior segment OCT based on multilevel deep network. *IEEE Trans. Cybern.* **50**, 3358–3366 (2020).
7. Friedman, D. S. & He, M. Anterior chamber angle assessment techniques. *Surv. Ophthalmol.* **53**, 250–273 (2008).
8. Lavanya, R. et al. Screening for narrow angles in the Singapore population: evaluation of new noncontact screening methods. *Ophthalmology* **115**, (2008).
9. Aung, T., Ang, L. P., Chan, S. P. & Chew, P. T. K. Acute primary angle-closure: Long-term intraocular pressure outcome in Asian eyes. *Am. J. Ophthalmol.* **131**, 7–12 (2001).
10. Zhao, J. et al. Phaco-goniosynechialysis versus phaco-trabeculectomy in patients with refractory primary angle-closure glaucoma: a comparative study. *BMC Ophthalmol* **23**, (2023).
11. Bernardes, R., Serranho, P. & Lobo, C. Digital ocular fundus imaging: a review. *Ophthalmologica* **226**, 161–181 (2011).
12. Panwar, N. et al. Fundus photography in the 21st Century–A review of recent technological advances and their implications for worldwide healthcare. *Telemed J. E Health.* **22**, 198–208 (2016).
13. Zhang, Z. et al. A survey on computer aided diagnosis for ocular diseases. *BMC Med. Inf. Decis. Mak* **14**, (2014).
14. Schober, P. & Schwarte, L. A. Correlation coefficients: appropriate use and interpretation. *Anesth. Analg.* **126**, 1763–1768 (2018).
15. Nahm, F. S. Receiver operating characteristic curve: overview and practical use for clinicians. *Korean J. Anesthesiol.* **75**, 25–36 (2022).
16. Liang, Y. et al. Prevalence and characteristics of primary angle-closure diseases in a rural adult Chinese population: the Handan eye study. *Investig Ophthalmol. Vis. Sci.* **52**, 8672–8679 (2011).
17. Tham, Y. C. et al. Global prevalence of glaucoma and projections of glaucoma burden through 2040: A systematic review and meta-analysis. *Ophthalmology* **121**, 2081–2090 (2014).
18. Campbell, P., Redmond, T., Agarwal, R., Marshall, L. R. & Evans, B. J. W. Repeatability and comparison of clinical techniques for anterior chamber angle assessment. *Ophthalmic Physiol. Opt.* **35**, 170–178 (2015).
19. Park, S. B. et al. Assessment of narrow angles by gonioscopy, Van Herick method and anterior segment optical coherence tomography. *Jpn J. Ophthalmol.* **55**, 343–350 (2011).
20. Choudhari, N. S., Chanda, S., Khanna, R., Senthil, S. & Garudadri, C. S. Diagnostic accuracy of Van Herick technique to detect Pre-Disease States of primary angle closure glaucoma in a resource constraint region. *Ophthalmic Epidemiol.* **26**, 175–182 (2019).
21. Zhang, Y., Li, S. Z., Li, L., Thomas, R. & Wang, N. L. The Handan eye study: comparison of screening methods for primary angle closure suspects in a rural Chinese population. *Ophthalmic Epidemiol.* **21**, 268–275 (2014).
22. Devereux, J. G. et al. Anterior chamber depth measurement as a screening tool for primary angle-closure glaucoma in an East Asian population. *Arch. Ophthalmol. (Chicago, Ill.)* 118, 257–263 (2000). (1960).
23. Xu, B. Y. et al. Ocular biometric determinants of anterior chamber angle width in Chinese americans: the Chinese American eye study. *Am. J. Ophthalmol.* **220**, 19–26 (2020).
24. Nolan, W. P. et al. Detection of narrow angles and established angle closure in Chinese residents of singapore: potential screening tests. *Am. J. Ophthalmol.* **141**, 896–901 (2006).
25. Norrby, S. Sources of error in intraocular lens power calculation. *J. Cataract Refract. Surg.* **34**, 368–376 (2008).
26. Chen, D. et al. Machine learning-guided prediction of central anterior chamber depth using slit lamp images from a portable smartphone device. *Biosensors* 11, (2021).
27. Qian, Z. et al. Detection of shallow anterior chamber depth from two-dimensional anterior segment photographs using deep learning. *BMC Ophthalmol* **21**, (2021).

28. Moghimi, S., Ramezani, F., He, M., Coleman, A. L. & Lin, S. C. Comparison of anterior segment-optical coherence tomography parameters in phacomorphic angle closure and acute angle closure eyes. *Investig Ophthalmol. Vis. Sci.* **56**, 7611–7617 (2015).
29. Ting, D. S. W. et al. Development and validation of a deep learning system for diabetic retinopathy and related eye diseases using retinal images from multiethnic populations with diabetes. *JAMA* **318**, 2211–2223 (2017).
30. Gulshan, V. et al. Development and validation of a deep learning algorithm for detection of diabetic retinopathy in retinal fundus photographs. *JAMA* **316**, 2402–2410 (2016).
31. Da Soh, Z. et al. From 2 dimensions to 3rd dimension: quantitative prediction of anterior chamber depth from anterior segment photographs via deep-learning. *PLOS Digit. Heal* **2**, (2023).

Acknowledgements
This study was entirely funded by the Shenyang Science and Technology Bureau, China(22-321-33-88). Supported by the project (Study on ACD classification of portable cell phone sword-lamp images to predict the risk of corner closure).

Author contributions
This thesis was mainly completed by the first author and assisted by other authors. Jiahui Zhao wrote the main article, Huixin Che and Xingru He supervised the revision of the article, Chenguang Zhang, Xin Zhang and Yiting Gong collected the data, and Guangzheng Dai, Shenming Hu, Guanghao Qin, Yibing Zhou and Shi Chen assisted in the writing of the article. All authors have read and approved the manuscript.

Funding
This study was funded entirely by the Shenyang Science and Technology Bureau, China(22-321-33-88). This project supported the ACD classification of portable cell phone sword-lamp images to predict the risk of corner closure.

Patient consent for publication

Competing interests
The authors declare no competing interests.

Informed consent
was obtained directly from the patients.

Ethics approval
The study protocol was approved by the Ethics Committee of He Eye Specialist Hospital (IRB (2022) K026.01) and adhered to the tenets of the Declaration of Helsinki. All subjects signed informed consent forms before they participated in the study. Written informed consent was obtained from the patients to publish any accompanying images. This manuscript includes no identifiable patient information.

Additional information
Correspondence and requests for materials should be addressed to H.C.